Journal of the European Ceramic Society **10** (1992) 263–271

Processing of Ceramic-Matrix/Platelet Composites by Tape Casting and Lamination

Thomas Claaßen & Nils Claussen

Technische Universität Hamburg-Harburg, Advanced Ceramics Group, D-2100 Hamburg 90, Germany

(Received 18 December 1991; accepted 30 April 1992)

Abstract

Composites with Al_2O_3 matrix and oriented SiC platelets were fabricated by tape casting and lamination. Suitable slips have been developed to obtain a homogeneous distribution of the components and a high degree of platelet orientation. The orientation has been improved by optimizing slip properties and by modifying the shape of doctor blades. The mechanical properties of laminates with different platelet sizes and contents have been determined. The highest fracture toughness (6·8 MPa $\sqrt{m}$) is exhibited by samples with 15 vol.% SiC platelets (3–20 μm). These composites have a bending strength of 370 MPa.

Verbundwerkstoffe mit Al_2O_3-Matrix und ausgerichteten SiC-Platelets wurden durch Tape Casting und Laminieren hergestellt. Dazu wurden geeignete Schlicker entwickelt, in denen die Komponenten homogen dispergiert sind und die beim Gießen eine möglichst gute Ausrichtung der Platelets liefern. Verbessert wurde die Ausrichtung durch die Optimierung der Schlicker und durch Modifikation der Schneidengeometrie beim Gießen. Die mechanischen Eigenschaften von Laminaten mit verschiedenen Plateletgrößen und -gehalten wurden bestimmt. Die höchste Bruchzähigkeit (6·8 MPa $\sqrt{m}$) wurde an Proben mit 15 Vol.% SiC-Platelets (3–20 μm) gemessen. Diese Proben haben eine Biegefestigkeit von 370 MPa.

Des matériaux composites avec une matrice d'alumine et des platelets de SiC orientés ont été fabriqués par coulage en bande et par laminage. Des lames adaptées ont été developpées pour obtenir une distribution homogène des composants et un haut degré d'orientation des platelets. L'orientation a été améliorée en optimisant les lames et modifiant la forme des lames de coulée. Les propriétées mécaniques d'échantillons laminés avec différentes tailles de platelets et différentes teneurs ont été déterminées. La plus grande résistance à la fracture (6·8 MPa $\sqrt{m}$) a été mesurée pour des échantillons contenant 15 vol.% de platelets de SiC (3–20 μm). Ces composites ont une résistance à la courbure de 370 MPa.

1 Introduction

The mechanical properties of ceramic materials can be improved by dispersing small, high-strength single crystals (whiskers, platelets, particles) in a ceramic matrix. Most investigations have been carried out on SiC-whisker toughening.[1] It is now known, however, that whiskers may pose a severe health hazard by inhalation of even small amounts.[2] An attractive alternative is given by platelet incorporation into brittle matrices.[3,4] Compared to whiskers, the advantages of platelets are their uncritical geometry which causes no health hazard, much lower price, higher thermal stability, and smoother and more perfect surfaces. On the other hand, the 'two dimensional' geometry of the platelets is disadvantageous for composites with randomly distributed toughening components. Densification to closed porosity of such composites by pressureless sintering is limited to a maximum platelet content of ~15 vol.%.[5,6] Usually, the loss of strength compared to the monolithic material is severe even for a small platelet content while the increase in toughness does not exceed 90%.[5,7,8] The strength of these composites is controlled by the size of the largest platelet cluster as the crack instability causing defect.

These intrinsic problems of platelet composites are thought to be minimized by fabricating com-

Journal of the European Ceramic Society 0955-2219/92/$5.00

posites with aligned platelets.[4] If the tensile stress axis is oriented parallel to the basal planes of platelets, only the thickness of the platelets (which is about 10 times less than their diameter) has to be considered as defect size. The inherent flaw size is larger in most cases. Models for toughening mechanisms in platelet composites have been calculated by Heußner.[5] A quantitative estimate of the toughness of zirconia (TZP) matrix composites with randomly distributed and oriented Al_2O_3-platelets predicts an optimum when most platelets are oriented with an inclination angle of about 1°–5° to the tensile stress axis. This estimate is based on a calculation of the crack closure stress due to the platelets as a function of platelet inclination angle.

The microstructural conditions for an optimized platelet composite can hence be summarized: high platelet aspect ratio, high platelet volume fraction, homogeneous platelet distribution, completely densified composite, and platelets closely oriented parallel to the tensile stress axis.[4,5]

This paper describes a method to fabricate composites with Al_2O_3-matrix and oriented SiC-platelets by tape casting and lamination. The influence of the processing parameters on the green density, fired density and platelet orientation have been investigated with special emphasis on the tape casting slip properties. Some mechanical properties have also been determined.

2 Experimental

2.1 Sample preparation

The processing of laminated platelet composites is summarized in Fig. 1. All materials (ceramic powders and organic additives) used for the experiments are from commercial sources (Table 1). SiC platelet grades SCP-F and SCP-M were wet sieved in isopropanol after ultrasonic deagglomeration through sieve sizes $<25\,\mu m$, 25–45 μm, 45–80 μm and $>80\,\mu m$.

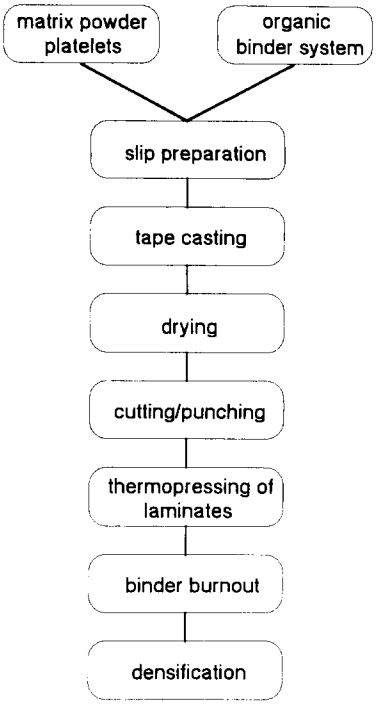

Fig. 1. Processing scheme for laminated platelet composites.

Slip preparation was carried out in a two-step procedure using a planetary ball mill with polyethylene containers and zirconia balls (20 mm dia.). The batch size was 200 g and the solid/solvent volume ratio was 0·35/0·65 for each slip. The first step was to deagglomerate the Al_2O_3 powder in a suspension with platelets, solvent, and a low content of dissolved organics at high milling speed for 4 hours. The second step was to homogenize the main part of the binder system with the well dispersed powder at low milling speed for 20 hours. The formulation for Al_2O_3 slips which was the basis for the investigations on slips containing Al_2O_3 and SiC platelets is given in Table 2.

Table 1. Materials for tape casting slips

Material	*Grade*	*Supplier*
Ceramic powders		
Al_2O_3	Ceralox APA-0.5	Condea Chemie, Hamburg, Germany
SiC-platelets	SCP-SF (3–20 μm)	C-Axis Technology, Montreal, Canada
SiC-platelets	SCP-F (10–50 μm)	C-Axis Technology, Montreal, Canada
SiC-platelets	SCP-M (20–90 μm)	C-Axis Technology, Montreal, Canada
Organic additives		
Ethanol (ETHO)	99% + 1% MEK	Brenntag, Mülheim-Ruhr, Germany
Butanone (MEK)		E. Merck, Darmstadt, Germany
Alkylphosphate	MDIT	Hoechst AG, Frankfurt a.M., Germay
Poly(vinyl butyral)	B79	Monsanto, St. Louis (MO), USA
Poly(vinyl butyral)	B98	Monsanto, St. Louis (MO), USA
Poly(ethylene glycol)	PEG 300	E. Merck, Darmstadt, Germany
Dibutyl phthalate (DBP)		E. Merck, Darmstadt, Germany

Table 2. Formulation for 35 vol.% Al_2O_3 slips

Material	*Content*	*Function*	*Dispersing step*	*Denomination of partial systems*
Butanone (MEK)	65 vol.%	Solvent	1	S
Ethanol		Solvent	1	S
	Mass% relative to total solid content			
MDIT	0·3	Dispersant	1	D
B79	0·7	Binder	1	B1
B98	6·3	Binder	2	B2
PEG	3·5	Plasticizer	2	P1
DBP	2·9	Plasticizer	2	P2

Tape casting was carried out on a laboratory scale tape casting bench (built by ENSCI, Limoges, France) with a movable casting head (Fig. 2). Two different, namely angular-shaped and round-shaped (Fig. 3) sets of two precisely adjustable doctor blades were used. Tapes were cast on float glass. The dried tapes were cut into squares of 45 × 45 mm and stacked to laminates of 30 tapes. The laminates were pressed at temperatures between 120°C and 140°C with 50 MPa for 30 min. Optimum conditions for binder burnout were derived from thermogravimetrical measurements. Previous experiments have shown that the weight loss during binder burnout should not exceed 0·01 mass%/min to avoid delamination. For each binder system and volume content the burnout cycle had to be adapted individually. Burnout was carried out in a muffle furnace in air.

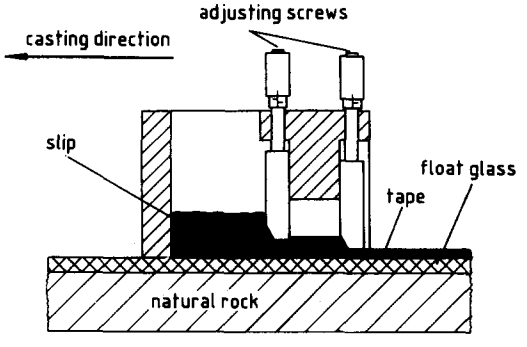

Fig. 2. Tape casting head.

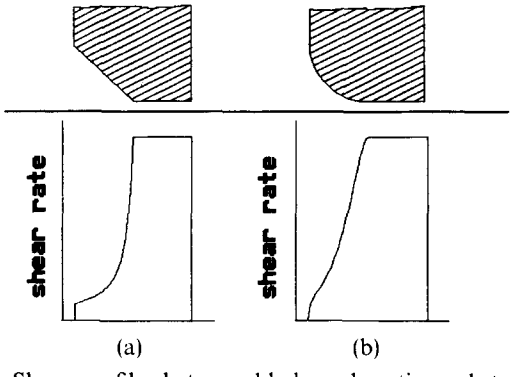

Fig. 3. Shear profiles between blade and casting substrate, (a) angular-shaped blade, (b) round-shaped blade, if a slip with Newtonian flow behaviour is cast without external pressure.

The laminated platelet composites and Al_2O_3 reference samples were densified by combined vacuum sintering and hot isostatic pressing in argon (sinter-HIP): 10 K/min to 1550°C, vacuum; 60 min, 1550°C, vacuum; 30 min, 1550°C, 200 MPa Ar, 10 K/min to 20°C.

2.2 Characterization

For rheological measurements, a computer aided Searle-type rotary viscosimeter (RV 20, Haake Meßtechnik, Karlsruhe, Germany) was used. The setting of flow curve experiments and shear jump experiments is shown in Table 3. The apparent viscosity η was measured at a shear rate of $\dot{\gamma} = 100\,s^{-1}$. Viscosities of partial slip formulations η_s and viscosities of the solvent with dissolved components η_{fl} were determined to calculate the relative viscosities η_{rel} and dispersion effectiveness δ for each organic slip component i as:

$$\eta_{rel} = \eta_s/\eta_{fl} \tag{1}$$

$$\eta_i = \log \eta_{rel}(i-1) - \log \eta_{rel}(i) \tag{2}$$

Densities of green tapes were determined geometrically by thickness measurements of the cut squares and are given without the organic content. Densities of laminates were determined geometrically after binder burnout and by the Archimedes method after sintering.

Flexural strength was measured in 4-point bending with 10 and 30 mm fixture spans. Fracture toughness was determined by the ISB method in 4-point bending.[9]

The orientation of platelets in laminates was measured by optical microscopy. First, the angular distributions of the long axes of platelets intersecting polished sections of two planes normal to the tape surfaces were measured. In a second step a scan of all possible spatial orientations of a plane was used to

Table 3. Parameters of rheological experiments

Flow curve						
Time (min)	1	3	4	3	4	3
Shear rate (s^{-1})	0	10	100	100	10	0
	Constant	Increase	Increase	Constant	Decrease	Decrease
Shear jump						
Time (min)	1	0	0·1	1	10	
Shear rate (s^{-1})	0	100	100	100	100	
	Constant	Jump	Constant	Constant	Constant	

estimate the spatial distribution of platelets. The scan points were represented by normals of planes and were equally distributed. For each plane the intersection angles with the two measuring planes were determined and its relative frequency was calculated as the product of the relative frequencies of the same measured angles. The spatial orientation angle ϑ is given with respect to the tape surfaces. The relative frequency of an orientation angle ϑ is derived by summing up the relative frequencies of all planes with this angle.

An exponential distribution function $\Phi(x)$ with the parameter a and the transformation:

$$x = \cos\vartheta \tag{3}$$

was fit by quasi-linear regression to the empirical frequency distribution of the orientation angle ϑ.

$$\Phi(x) = 1 - e^{-a \cdot x} \tag{4}$$

Accuracy and significance of this method were proved by model calculations. The parameter a is termed here orientation exponent.

3 Results and Discussion

3.1 Slip characteristics

Phosphate esters which have been investigated as dispersants for oxide powders are known to stabilize a powder suspension in nonaqueous media by electrostatic mechanisms.[10,11] Dispersion experiments with the Al_2O_3 powder described in Table 1 have shown that suspensions with a solid content of 35 vol.% exhibit strongly pseudoplastic flow behaviour and a minimum apparent viscosity of 2·4 Pas with an addition of 0·3 mass% phosphate ester (Table 1). This indicates that this powder is dispersed in a weakly flocculated structure which can be destroyed by shear forces. As shown in Fig. 4, the apparent viscosity of such suspensions can be decreased by small amounts of the poly(vinyl butyral) binder B79 (Table 1). A minimum viscosity of 0·8 Pas was determined for addition of 0·7% B79. According to results from Sacks & Scheiffele[12] the adsorption of poly(vinyl butyral) on Al_2O_3 powder surfaces leads to effective steric stabilisation.

A partial slip formulation SDB1 with a solid content of 35 vol.% Al_2O_3 and addition of 0·3% MDIT and 0·7% B979 is characterized by the flow curve (a) shown in Fig. 5. This flow curve exhibits two regions: increasing shear stress up to a shear rate of $10\,s^{-1}$ and nearly constant shear stress at shear rates $> 10\,s^{-1}$. We suppose that the adsorbed poly(vinyl butyral) molecules give rise to particle interaction when particle distances are small as they are with a mean particle distance of 417 nm in a 35 vol.% suspension of Al_2O_3 with a mean particle size of 320 nm. The observed change in flow behaviour at a shear rate of $10\,s^{-1}$ is related to a structural change

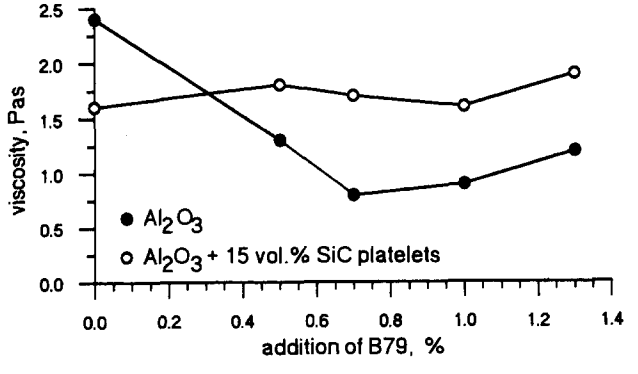

Fig. 4. Apparent viscosities of partial slip formulations (SDB1) as a function of B79 (B1) addition at a shear rate of $100\,s^{-1}$; SiC platelets: SCP-M 25–45 μm.

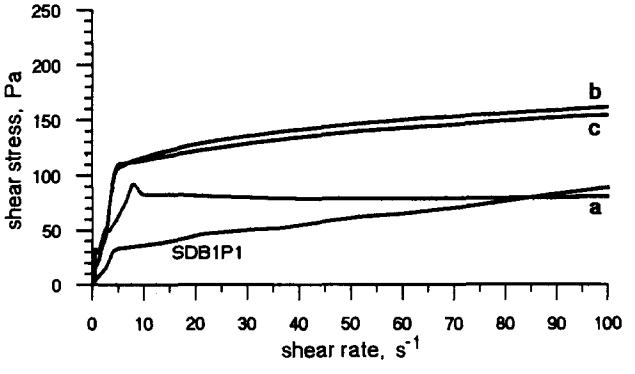

Fig. 5. Flow curves of partial slip formulations SDB1 with 35 vol.% solid, (a) Al_2O_3, (b) Al_2O_3 + 15 vol.% SiC platelets SCP-M 25–45 μm, (c) Al_2O_3 + 15 vol.% SiC platelets SCP-SF, and of a partial slip formulation SDB1P1 with the solid component (b).

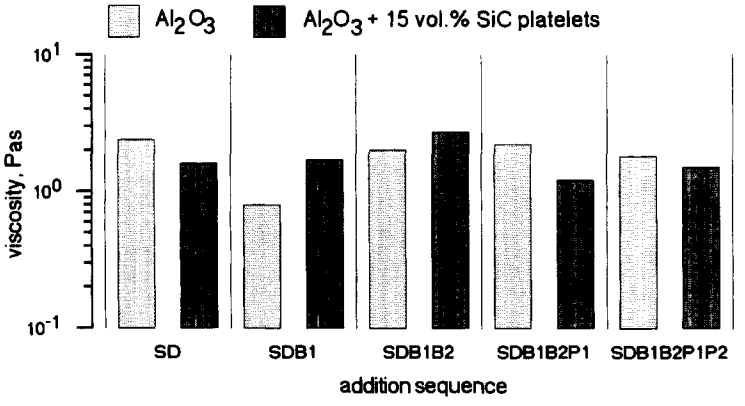

Fig. 6. Apparent viscosities of partial slip formulation with the addition sequence SDB1B2P1P2 at a shear rate of $100\,s^{-1}$.

of the suspension with a sharp decrease of particle interactions. As the flow curves (b) and (c) in Fig. 5 show, platelet containing suspensions SDB1 have a similar flow behaviour as Al_2O_3 suspensions but structural change occurs at the lower shear rate of $\sim 5\,s^{-1}$. This particular shear rate decreases slightly with increasing platelet volume content. Increasing mean distance between matrix powder particles with increasing platelet content can explain this result. The flow behaviour is nearly unaffected by the platelet size.

Addition of phosphate ester to a suspension of Al_2O_3 powder and SiC platelets yields a lower apparent viscosity of 1·6 Pas compared to 2·4 Pas of Al_2O_3 suspensions but in contrast to this the apparent viscosity is nearly unaffected by the addition of poly(vinyl butyral) (Fig. 4). We suppose that competitive adsorption both on powder and platelet surfaces decreases the amount of poly(vinyl butyral) available for stabilizing the matrix powder. Compared to Al_2O_3 suspensions, platelet containing suspensions exhibit a higher shear stress gradient at high shear rates, which indicates that platelets act as flow hindrance.

The apparent viscosities of partial slip formulation for the addition sequence SDB1B2P1P2 are shown in Fig. 6. Al_2O_3 slips exhibit the lowest viscosity of 0·8 Pas after the first dispersion step (SDB1) while a suspension SDB1 with 85 vol.% Al_2O_3 and 15 vol.% SiC-Platelets has an apparent viscosity of 1·6 Pas. The calculated dispersion effectiveness (eqn 2) for each component is given in Table 4. If the solid component consists of 15 vol.% SiC platelets the dispersion effectiveness of B1 is reduced from 1 to 0·5. Since a well dispersed suspension should be obtained after the first dispersion step to yield homogeneous packing in the tape it is useful to add another slip component with a positive dispersion effectiveness to the first dispersion step. The apparent viscosities for partial slip formulations of a 85 vol.% Al_2O_3/15 vol.% SiC platelet slip with changed addition sequence SDB1P1B2P2 are shown in Fig. 7. Now the lowest viscosity is obtained after the first dispersion step (SDB1P1) with 0·9 Pas. As shown in Fig. 5 the flow characteristic has not changed after addition of P1 (plasticizer PEG) but the flow curve is shifted towards lower shear stresses. The shear stress at the point of structural change (shear rate of $5\,s^{-1}$) decreases from 110 to 35 Pa. Hence, the plasticizer reduces the interparticle forces by interactions with the adsorbed poly(vinyl butyral). Since the dispersion effectiveness values for the addition sequence SDB1P1B2P2 (Table 4) do not differ significantly

Table 4. Dispersion effectiveness δ of organic additives in slips of Al_2O_3 and Al_2O_3 + 15 vol.% SiC-platelets (SCP-M 25–45 μm), 35 vol.% solid, 65 vol.% MEK-ETHO, +0·3% MDIT, with different addition sequences (sequ.)

Additive i	*Mass % related to total solid content*	*Addition sequence*		
		SDB1B2P1P2		*SDB1P1P2B2*
		Al_2O_3 δ_i	$Al_2O_3 + 15SiC$ δ_i	$Al_2O_3 + 15SiC$ δ_i
B1 (B79)	0·7	1·00	0·50	0·50
B2 (B98)	6·3	1·43	1·62	1·54
P1 (PEG)	3·5	−0·04	0·35	0·34
P2 (DBP)	2·9	0·09	−0·10	−0·01

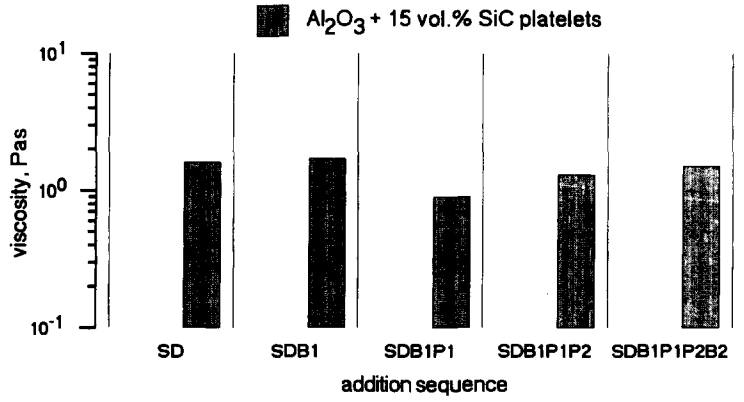

Fig. 7. Apparent viscosities of partial slip formulation with the changed addition sequence SDB1P1B2P2 at a shear rate of $100\,s^{-1}$.

from the previous values, obviously no chemical reactions take place depending on the addition sequence during the dispersion procedure.

Flow curves of platelet containing slips with 0·7%, 1·0%, and 1·3% B79 are nearly identical but different behaviour in a shear jump experiment was observed. Slips with 0·7% B79 respond to a rapidly increasing shear rate with a viscosity increase by a factor 10 decreasing to a constant value within 2 min (Fig. 8). This behaviour was not found for slips with 1·0 and 1·3% B79. Since similar rapid shear rate increases occur when the slip passes the blades during tape casting, the viscosity-time behaviour of a shear jump may influence the quality of cast tapes. This was verified both by the green densities and by the platelet orientation measured at tapes and laminates from different slip formulations (Table 5).

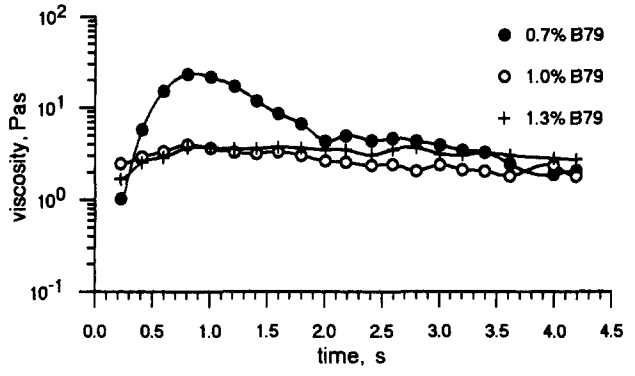

Fig. 8. Apparent viscosity vs. time of slips containing Al_2O_3 + 15 vol.% SiC platelets (SCP-SF) after a shear jump to a shear rate of $100\,s^{-1}$.

Table 5. Green densities (with standard deviation) of tapes and platelet orientation exponent from laminates containing Al_2O_3 + 15 vol.% SiC-platelets (SCP-SF)

Addition of B79 mass%	*Relative density*	*Orientation exponent*
0·7	0·579 (0·016)	3·4
1·0	0·614 (0·012)	4·6
1·3	0·615 (0·017)	—

Tapes cast from slips with 0·7% B79 exhibit a significantly lower green density and a broader distribution of the orientation angle (Fig. 9). Tapes cast from slips with 1·3% B79 also exhibit high green densities but are too brittle for further handling.

3.2 Tape casting and lamination

The slip undergoes a rapid shear rate increase when it passes the blades controlled by the blade geometry and flow behaviour of the slip. These conditions could not be simulated with the rheometer used because the period in which the slip is sheared is too small, but it was assumed that all platelet containing slips respond to a shear jump with an elevated viscosity. Only the relaxation time depends on the slip components (it was not measurable for slips with $\geq$ 1·0% B79 in the experiment reported above).

As shown in Fig. 10, substantial improvements in platelet orientation were made when a round-shaped blade was used instead of an angular-shaped blade. The orientation exponent was raised from 4·6 to 6·0 for laminates with 15 vol.% SiC-platelets of SCP-SF grade (Table 1). Misorientation of platelets may be caused by the discontinuous shear rate gradient between an angular-shaped blade and the casting substrate (Fig. 3). Instead, round-shaped blades cause rapid but continuous shear rate increase.

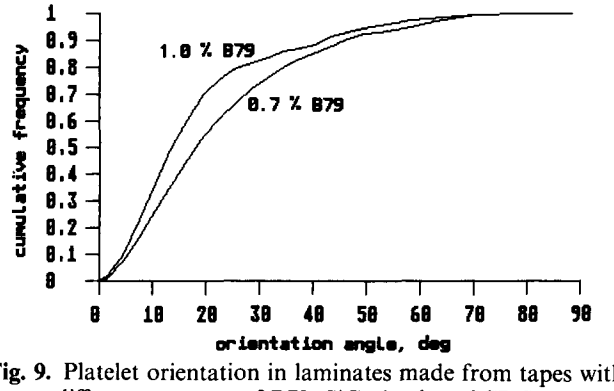

Fig. 9. Platelet orientation in laminates made from tapes with different contents of B79; SiC platelets: SCP-SF.

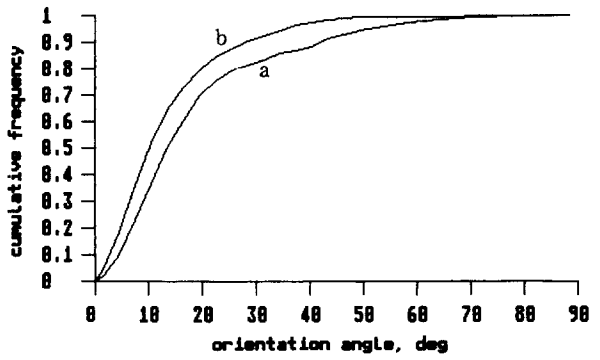

Fig. 10. Platelet orientation in laminates made from tapes which were cast with the two different blades shown in Fig. 3; SiC platelets: SCP-SF.

Two sources of composite delamination defects can be reduced by an optimized thermocompression cycle: insufficient binder flow during thermocompression and gas bubbles between the tapes. Gas bubbles are removed by stepwise buildup to maximum pressure with complete decompression before each step. Since binder flow under pressure is disturbed by platelets, the maximum temperature must be raised to just below a value where plastic deformation of the laminate occurs. This temperature can be obtained from the piston compliance upon heating. When plastic deformation starts, the temperature must be reduced slightly. With this method, delamination defects have been reduced substantially. The maximum temperature of a thermocompression cycle increases with increasing platelet content and size (Fig. 11).

3.3 Microstructure and mechanical properties

Platelet distribution and orientation in a laminated composite is shown in Fig. 12. The orientation exponent depends significantly on the platelet size. The values measured from laminates with 15 vol.% of different platelet grades (Table 1) are: 3.3 (SCP-M, 45–80 μm), 4·1 (SCP-M, 25–45 μm), 4·3 (SCP-F, <25 μm), and 6·0 (SCP-SF). The empirical angular distributions are shown in Fig. 13. Platelet orientation is not influenced by the platelet volume content (Fig. 14).

Fired densities of laminate composites are shown in Fig. 15. Densification to closed porosity was achieved with a platelet content up to 15 vol.% of grade SCP-SF and SCP-F, <25 μm and up to 20 vol.% of grade SCP-M, 25–45 μm respectively. These samples exhibit continuously decreasing density with increasing platelet content and size which can be explained by models of constrained

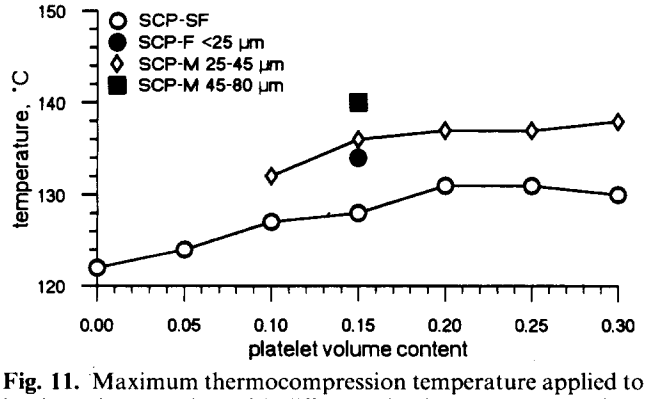

Fig. 11. Maximum thermocompression temperature applied to laminated composites with different platelet contents and sizes.

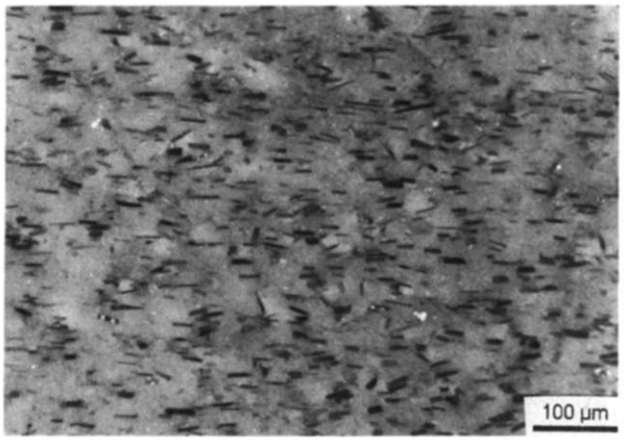

Fig. 12. Optical micrograph normal to the tape surfaces of a laminated platelet composite containing Al_2O_3 + 20 vol.% SiC platelets SCP-M 25–45 μm.

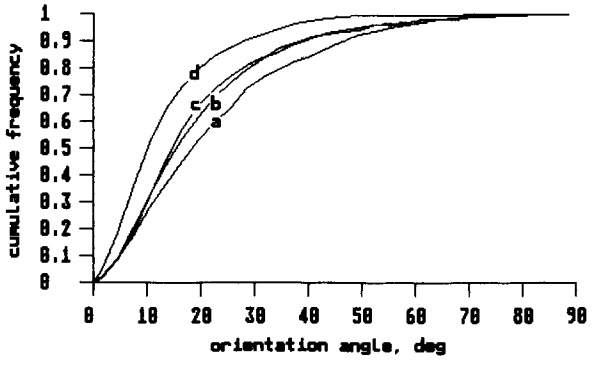

Fig. 13. Platelet orientation in laminates containing different platelet sizes; (a) SCP-M 45–80 μm, (b) SCP-M 25–45 μm, (c) SCP-F <25 μm, (d) SCP-SF.

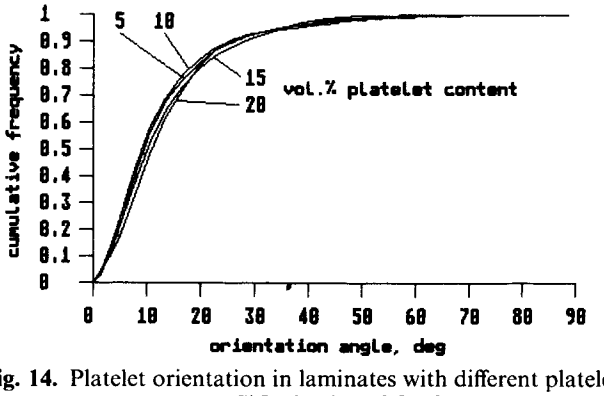

Fig. 14. Platelet orientation in laminates with different platelet contents; SiC platelets: SCP-SF.

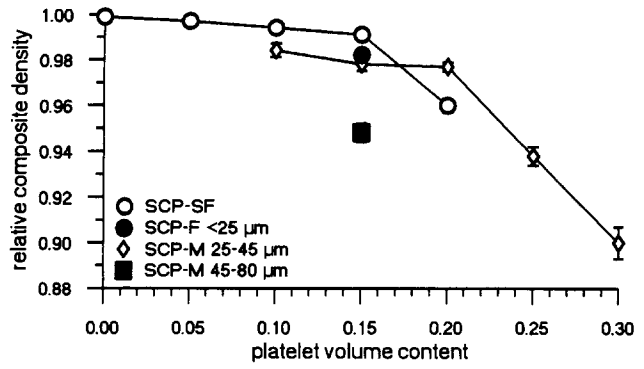

Fig. 15. Relative density of laminated Al_2O_3/SiC platelet composites with different platelet contents and sizes densified by sinter-HIP.

sintering with rigid inclusions.[13,14] Density increases with increasing orientation exponent. Complete densification was not achieved, even by hot isostatic pressing. Samples with 15 vol.% SCP-M 45–80 μm, 20 vol.% SCP-SF and more than 20 vol.% SCP-M 25–45 μm exhibit insufficient densification of the matrix (open porosity).

Flexural strength and fracture toughness are shown in Fig. 16 and Fig. 17. The strength as well as the toughness decrease with the platelet size. Even small amounts of platelets reduce the strength from a base value of 624 MPa to <450 MPa. The maximum fracture toughness at a platelet content of

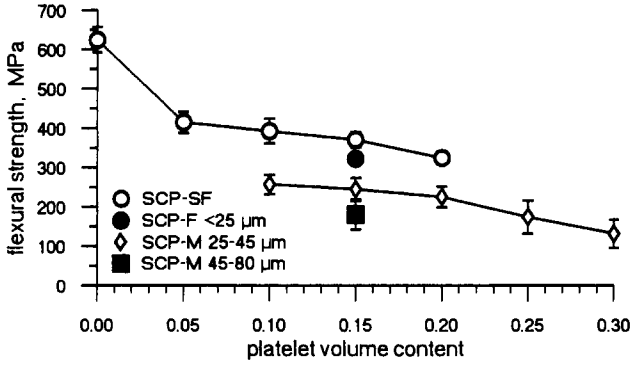

Fig. 16. Flexural strength of laminated Al_2O_3/SiC platelet composites with different platelet contents and sizes.

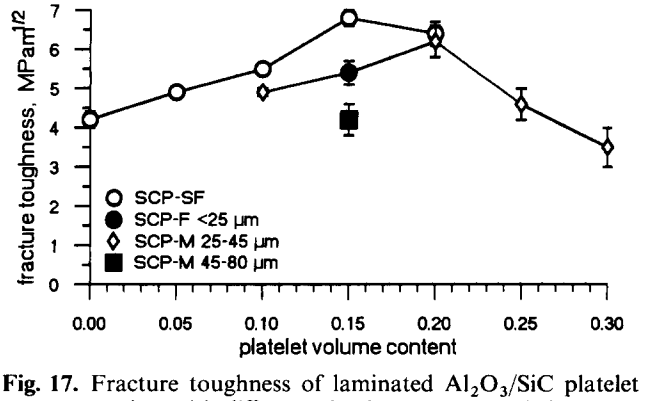

Fig. 17. Fracture toughness of laminated Al_2O_3/SiC platelet composites with different platelet contents and sizes.

15 vol.% (6·8 MPa $\sqrt{m}$) for SCP-SF and 20 vol.% (6·2 MPa $\sqrt{m}$) for SCP-M 25–45 μm, respectively, can be correlated to the density values, hence these platelet contents represent the limits for densification to closed porosity. The maximum fracture toughness increase (6·8 MPa $\sqrt{m}$ compared to a base value of 4·2 MPa $\sqrt{m}$) was obtained with the smallest platelet fraction.

4 Conclusions

1. Multilayer composites with oriented platelets can be fabricated by tape casting and lamination.
2. Optimum orientation is achieved with the smallest platelet fraction (3–20 μm) where 50% of the platelets are oriented with an angle $< 10°$ to the tape surface.
3. The degree of orientation is improved with a special blade geometry leading to a continuously increasing shear rate.
4. Internal flaws are reduced by an improved lamination technique that allows an individual adaptation of the thermocompression temperature to each composite composition.
5. Constraint of densification by platelet inclusions is reduced with increasing degree of platelet orientation.
6. Fracture toughness increases with increasing platelet content if the composite is densified to closed porosity.

Acknowledgement

The authors thank BMFT for financial support which has been part of the BMFT joint project No. 03 M 1023.

References

1. Becher, P. F., Microstructural design of toughened ceramics. *J. Am. Ceram. Soc.*, **74** (1991) 255–69.
2. Birchall, J. D., Stanley, D. R., Mockford, M. J., Pigott, G. H. & Pinto, G. J., Toxicity of silicon carbide whiskers. *J. Mater. Sci. Lett.*, **7** (1988) 350–2.
3. Böcker, W. G. D., Chwastiak, S., Frechette, F. & Lau, S.-K., Single-phase alpha-SiC reinforcements for composites. In *Silicon Carbide '87, Ceramic Transactions, 2*, ed. J. D. Cawley & C. E. Semler. Am. Ceram. Soc., Westerville, OH, 1989, pp. 407–20.
4. Claussen, N., Ceramic platelet composites. In *Structural Ceramics—Processing, Microstructure and Properties*, eds J. J. Bentzen *et al.* Risø National Laboratory, Roskilde, 1990, pp. 1–12.
5. Heußner, K.-H., Mechanische Eigenschaften von ZrO_2

(TZP)/Al_2O_3-Platelet-Verbundwerkstoffen. *Fortschrittberichte VDI, Series* 5. Grund- und Werkstoffe, Nr. 225, VDI, Düsseldorf, 1991.
6. Claaßen, T. & Claussen, N., Processing routes and microstructure of ceramic-matrix/platelet composites. In *4th International Symposium on Ceramic Materials and Components for Engines*, eds R. Carlsson, T. Johansson & L. Kahlman. Elsevier, London, 1992, pp. 715–25.
7. Baril, D. & Jain, M. K., Evaluation of SiC platelets as a reinforcement for oxide matrix composites. *Ceram. Eng. Sci. Proc.*, **12** (1991) 1175–92.
8. Nischik, C., Seibold, M. M., Travitzky, N. A. & Claussen, N., Effect of processing on mechanical properties of platelet-reinforced mullite composites. *J. Am. Ceram. Soc.*, **74** (1991) 2464–8.
9. Chantikul, P., Anstis, G. R., Lawn, B. R. & Marshall, D. B., A critical evaluation of indentation techniques for measuring fracture toughness: II. Strength method. *J. Am. Ceram. Soc.*, **64** (1981) 539–44.
10. Chartier, T., Streicher, E. & Boch, P., Phosphate esters as dispersants for tape casting alumina. *Am. Ceram. Soc. Bull.*, **66** (1987) 1653–5.
11. Cannon, W. R., Morris, J. R. & Mikeska, K. R., Dispersants for nonaqueous tape casting. In *Advances in Ceramics 19, Multilayer Ceramic Devices*, eds J. B. Blum & W. R. Cannon. Am. Ceram. Soc., Westerville, OH, 1986, pp. 161–74.
12. Sacks, M. D. & Scheiffele, G. W., Polymer adsorption and particulate dispersion in nonaqueous Al_2O_3 suspensions containing poly(vinyl butyral) resins. In *Advances in Ceramics 19, Multilayer Ceramic Devices*, eds J. B. Blum & W. R. Cannon. Am. Ceram. Soc., Westerville, OH, 1986, pp. 175–84.
13. Tuan, W. H., Gilbart, E. & Brook, R. J., Sintering of heterogeneous ceramic compacts. Part 1: Al_2O_3–Al_2O_3. *J. Mater. Sci.*, **24** (1989) 1062–8.
14. Lange, F. F., Constrained network model for predicting densification behavior of composite powders. *J. Mater. Res.*, **2** (1987) 59–65.